Astronomy & Astrophysics manuscript no. art
February 16, 2012

© ESO 2012

arXiv:1202.3346v1 [astro-ph.CO] 15 Feb 2012

Gravitational wave background from population III binaries

I. Kowalska[1], T. Bulik[1], and K. Belczynski[1,2]

[1] Astronomical Observatory, University of Warsaw, Al Ujazdowskie 4, 00-478 Warsaw, Poland
[2] Dept. of Physics and Astronomy, University of Texas, Brownsville, TX 78520, USA

Received ; accepted

ABSTRACT

Context. The current star formation models imply that the binary fraction of population III stars is non zero. The evolution of such binaries must have led to formation of compact object binaries.
Aims. In this paper we estimate the gravitational wave background originating in such binaries and discuss its observability .
Methods. The properties of the population III binaries are investigated using a binary population synthesis code. We numerically model the background and we take into account the evolution of eccentric binaries.
Results. The gravitational wave background from population III binaries dominates the spectrum below 100 Hz. If the binary fraction is larger than 10^{-2} the background will be detectable by LISA and DECIGO.
Conclusions. Gravitational wave background from population III binaries will dominate the spectrum below 100 Hz. LISA, ET and DECIGO should either see it easily or, in case of non detection, provide very strong constraints on the properties of the population III stars.

Key words. binaries – gravitational waves

1. Introduction

Coalescing compact object binaries are the most promising sources of gravitational waves. This include the double neutron star binaries (DNS), the mixed, black hole neutron star binaries (BHNS) and binary black holes (BBH). Gravitational wave signal may be detected as single events from nearby sources, however for the distant ones the signals will overlap contributing to gravitational wave background (GWB). GWB from coalescing compact object binaries has been investigated by numerous authors (e.g., Tumlinson & Shull 2000; Bromm et al. 2001; Rosado 2011; Zhu et al. 2011; Olmez et al. 2011; Regimbau 2011; Marassi et al. 2011). The existing gravitational wave detectors LIGO and VIRGO have achieved their design sensitivity (Accadia et al. (2011), Kawabe & the LIGO Collaboration (2008)). Currently they are undergoing transitions to the Advanced phase with the sensitivity increased by a factor 30. Additionally there are plans to construct other large scale detectors such as LCGT (Kuroda & LCGT Collaboration 2010). In a more distant future third generation detector like the Einstein Telescope (ET) (Van Den Broeck 2010) should be constructed. Theses instrumental developments make the investigation of stochastic backgrounds of gravitation waves very important. We expect that at lower frequencies such as designed band of ET ($\sim$ 1Hz), large population of distant object will be observed. The biggest contribution in that frequency window will come from massive BBH. There are no direct observations of that kind of objects, therefore there are many uncertainties in stellar evolution models leading to creation BBH. Because of the range of future detectors there is possibility that among observed objects could be the remnants of the oldest stars in the Universe. Population III stars should be metal free, therefore they should produce black holes of masses reaching hundreds solar masses. If our understanding of their evolution is correct, there should be significant gravitational background from remnants of population III stars.

In this paper we investigate the possible contribution to the GWB from population III star binaries. Population III stars are the first stars in the Universe that formed out of metal free material. As such, they had very different properties than the currently forming stars. The evolution and properties of single Population III star have been investigated by Baraffe et al. (2001), Tan (2008). They found that the single population III star are stable up to a few hundred solar masses. Moreover they evolve with a little mass loss. The evolution of such massive star will end up either in a pair instability supernova leaving no remnant, or forming a black hole through a direct collapse. While no population III stars are known, their properties have been investigated by numerical simulations of the collapse of metal free clouds of gas. These simulations have shown that the initial mass function of population III star is skewed towards higher masses than the one on the population I or II stars (Abel et al. 2002; Bromm et al. 2002). The existence of binaries among Population III star has been uncertain, however simulations of collapse of rotating clouds of gas have shown bar instabilities and formation of two protostars (Saigo et al. 2004; Machida et al. 2008). Since all known stellar populations contain a significant fraction of binaries, it seems justified to consider the properties of Population III binaries. The evolution of Population III binaries has been investigated by Belczynski et al. (2004) and Kulczycki et al. (2006). They found that coalescence of BBH binaries originating in population III stars may be a significant source of gravitational waves for the current and future gravitational wave interferometers. In section 2 we analyze the gravitational wave spectrum form eccentric binaries, section 3 is devoted to the analysis of properties of population III binaries. Section 4 contains an outline of the estimate of the GWB. We present the results in section 5 and in section 6 we discuss them.

2. Population of Pop. III stars - models

The evolution of population III metal free stars was first examined in detail about ten years ago Heger et al. (2001), Baraffe et al. (2001), Marigo et al. (2001), Marigo et al. (2003), Schaerer (2002). It was found that such stars are stable with masses up to 500 $M_{\odot}$. Population III star evolve very quickly with nearly no mass loss. Depending on the initial mass they may form neutrons stars, black holes or leave no remnant at all, because of total star disruption in pair instability supernova (Heger & Woosley 2002). The mass spectrum of population III stars is still a matter of a debate. On one hand the simulations of metal free cloud collapse indicate the possibility of forming high mass objects. The searches for low mass metal free stars that should still be around brought no success, which indicates that the low mass cutoff of population III initial mass function was significantly higher than for the current population of stars. An additional question is whether population III stars also were formed as binaries. Every known stellar population contains a significant fraction of binaries, so one should also expect this to be the case for population III stars. Numerical simulations of collapse of rotating metal free clouds indicate appearance of a bar instability which leads to formation of two protostars in a binary (Saigo et al. 2004). In a recent simulations (Turk et al. 2009; Stacy et al. 2010; Greif et al. 2011; Clark et al. 2011; Stacy et al. 2012) a similar result was shown. A massive protostellar cloud develops spiral structure, instabilities and leads to formation of several multiple systems. Thus we conclude that there is ample evidence to allow investigation of population III binary evolution and it consequences.

We model the evolution of population III binaries using a code described in Belczynski et al. (2004). The code uses the evolutionary sequences based on Heger et al. (2001), Baraffe et al. (2001), Marigo et al. (2001). It includes a detail treatment of the calculation of stellar remnants. The binary evolution calculation involves analysis of stability of mass transfers. The common envelope mass transfers end in a merger if the donor is a main sequence star and for giant stars we use the standard formalism of Webbink (1984).

We assume that the initial mass function of the primaries stretches between 10 and 500 $M_{\odot}$ with the exponent of -2.35. The mass ratio is drawn from a flat distribution. The initial orbital separation distribution is flat in logarithm of a. The range of initial orbital separation is bounded from below by the requirement that the stars are not in contact at zero age main sequence (ZAMS) - $a_{min} = 1.3(R_1 + R_2)$. The upper bound is more arbitrary. We have chosen $a_{max} = 10^6 R_{\odot}$. While Bromm & Loeb (2006) argue that the upper limit on initial separation is as large as $5 \times 10^7 R_{\odot}$, we wanted to include all systems that interact. The binaries with initial separations close to or above our upper limit will not interact and if they survive the evolution and form compact object binaries, they will only contribute to the GW background spectrum below 10^{-11}Hz. The uncertainty in the number of binaries due to variation of the upper cutoff a_{max} is small because of logarithmic distribution of initial orbital separations. We calculate the evolution of binaries and note that cases when a compact object binary was formed. Then we trace it evolution due to emission of gravitational waves.

2.1. Properties of compact objects

We evolved 10^6 binary stars of zero metallicity using population synthesis code `StarTrack`. As a result we obtained 462496 compact objects, which we treat as a realistic sample of population III remnants. More than 60% of them are BBH systems, where both components have masses greater than $2.5 M_{\odot}$. Detailed distributions of initial parameters are presented on Figure 2.1. On the top panel one can see that there is very broad range of initial eccentricities - over 60% of all binaries have eccentricity greater than 0.1. Bottom panel shows distributions of chirp masses and coalescence times. Only 12% of binaries will merge within present Hubble time.

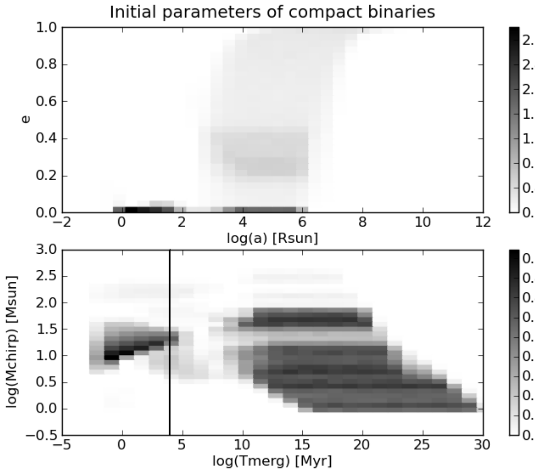

Fig. 1. The initial properties of the Population III compact object binaries. The top panel shows the distribution of the orbital properties, ie. the density in the plane spanned by the semi-major axis and the eccentricity of the orbit. The lower panel shows the distribution of the chirp masses and the merger times of the binaries. Vertical line represents Hubble time. Numbers represent percentage of all binaries in simulation.

3. Gravitational wave spectrum of eccentric binaries

While the spectrum from circular binaries is well known, we have shown above that a large fraction of population III binaries will be eccentric. It is therefore important to investigate the possible effects of eccentricity on the gravitational wave spectra of compact object binaries. (Peters & Mathews 1963; Peters 1964)

3.1. General derivation

The gravitational wave spectrum from a binary can be calculated as:

$$\frac{dE_{gw}}{df_{gw}} = \frac{dE_{gw}}{dt}\left(\frac{df_{gw}}{dt}\right)^{-1} \tag{1}$$

The velocity on an eccentric orbit is changing over its period, therefore the instantaneous orbital frequency is also varying. Thus the system is radiating in some range of frequencies, not just in one particular, like in the case of a circular orbit.

In the quadrupole approximation the orbit decays due to gravitational wave emission and the orbital parameters change as:

$$\frac{da}{dt} = -\frac{64}{5}\frac{G^3 \mu M^2}{a^3 c^5}\Psi(e), \tag{2}$$

$$\Psi(e) = \frac{1 + 73/24 e^2 + 37/96 e^4}{(1-e^2)^{7/2}}. \tag{3}$$

while orbital frequency is

$$f_{orb} = \frac{1}{2\pi}\left(\frac{GM}{a^3}\right)^{1/2}. \tag{4}$$

where we denoted the total mass of the binary M, μ is the reduced mass, and a is the semi-major axis. An eccentric binary emits gravitational waves in a spectrum of harmonics of the orbital frequency

$$f^n_{gw} = n f_{orb}, \tag{5}$$

$$\frac{d f_{gw}}{dt} = n\frac{d f_{orb}}{dt}. \tag{6}$$

In the case of circular orbit gravitational waves are emitted only in one mode $n = 2$. Inserting equations 4 and 2 into equation 6 we obtain:

$$\frac{d f^n_{gw}}{dt} = \frac{96}{5}\left(\frac{2\pi}{n}\right)^{8/3}\frac{f^{n\ 11/3}_{gw} G^{5/3} M^{5/3}_{chirp}}{c^5}\Psi(e), \tag{7}$$

where we introduced the chirp mass, which is quantity that determines amplitude and frequency dependence of the inspiral gravitational wave signal. $M_{chirp} = \mu^{3/5}M^{2/5}$. The power of radiation for each harmonic was calculated by Peters & Mathews (1963):

$$\frac{dE}{dt}(n) = \frac{32}{5}\frac{G^4\mu^2M^3}{c^5a^5}g(n,e), \tag{8}$$

where $g(n,e)$ is:

$$\begin{aligned} g(n,e) \ = \ & \frac{n^4}{32}\left\{[J_{n-2}(ne) - 2eJ_{n-1}(ne) + \frac{2}{n}J_n(ne)\right. \\ & +2eJ_{n+1}(ne) - J_{n+2}(ne)]^2 \\ & +(1-e^2)\,[J_{n-2}(ne) - 2J_n(ne) + J_{n+2}(ne)]^2 \\ & \left. +\frac{4}{3n^2}\,[J_n(ne)]^2\right\} \end{aligned} \tag{9}$$

and J_n are the Bessel functions. This result follows from Fourier analysis of the Kepler motion Peters & Mathews (1963). We obtain the instantaneous spectrum of gravitational waves from an eccentric binary by combining equations 1- 8 and 7:

$$\frac{dE}{d f^n_{gw}} = \frac{\pi}{3}\frac{1}{G}\left(\frac{4}{n^2}\right)^{1/3}\frac{\left(GM_{chirp}\right)^{5/3}}{\left(f^n_{gw}\pi\right)^{1/3}}\frac{g(n,e)}{\Psi(e)}. \tag{10}$$

In the case of the circular orbit this reduces to the well known result, e.g. (Phinney 2001):

$$\left.\frac{dE}{d f_{gw}}\right|_{e=0} = \frac{\pi}{3}\frac{1}{G}\frac{\left(GM_{chirp}\right)^{5/3}}{\left(f_{gw}\pi\right)^{1/3}}, \tag{11}$$

since $\Psi(e = 0) = 1$, $g(n, e = 0) = 1$ when $n = 2$ and $g(n \neq 2, e = 0) = 0$. The result has to be averaged over the lifetime of the binary. In the following section we discuss two cases: the long lived and the short lived binaries, as outlined below.

3.2. Long-lived systems

By term long-living we mean that the time to coalescence is longer than present Hubble time, which we assume for simplicity $t_H = 10^4 Myr$. We are interested in objects that have not merged. Such objects have very wide orbits and the semi-major axis of the binary as well as its eccentricity can be assumed to be constant during the entire evolution time.

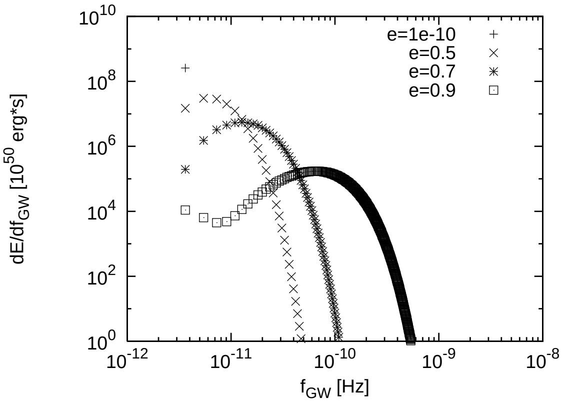

Fig. 2. Spectra of the GW radiation from long-living binary ($M_1 = M_2 = 300\,M_\odot$ $a = 1.2\times10^6\,R_\odot$) for different values of eccentricity. A single 'plus' mark corresponds to circular orbit, by crosses we show case for eccentricity 0.5, stars corresponds to eccentricity 0.7 and squares to initial eccentricity 0.9

In this case the spectrum is discrete as the binary emits the gravitational radiation only at the frequencies specified by the harmonics.

$$\frac{dE}{df} = \sum_{n=2}^{\infty}\delta(f - n f_{orb})\frac{dE}{d f^n_{gw}}, \tag{12}$$

where the spectrum in each harmonic is given by equation 10.

To illustrate this case we chose binary consisting of two massive black holes: $M_1 = M_2 = 300\,M_\odot$ on wide orbit $a = 1.2\times10^6\,R_\odot$. We present the spectra for a few values of the eccentricity in Figure 2.

When eccentricity is almost zero we have just one point - it corresponds to very wide, circular orbit. Velocity in that case is constant and we observe only one frequency. While eccentricity is increasing we observe that spectrum is wider. Also maximum of energy distribution is shifted to the higher frequencies. For the highest considered eccentricity (0.9), there is a minimum around frequency 10^{-11}. It is caused by the specific structure of the function described by equation 9.

3.3. Short-lived systems

In that group we consider systems which can coalescence during they evolution. The orbit is changing and we observe radiation in very wide range of frequencies. In this case the binary emits a continues spectrum over its lifetime. The orbital frequency changes from f_{ini} - the initial orbital frequency determined by the orbital parameters after formation of the second compact object in the binary, to the final orbital frequency just before merger. For the final orbital frequency we chose the frequency at the marginally stable orbit

$$f_{ISCO} = \frac{c^3}{6\sqrt{6}G(M_1+M_2)}. \tag{13}$$

As the binary evolves, its eccentricity decreases and the evolution of eccentricity can be found by solving the equation:

$$\frac{de}{d f_{orb}} = -\frac{19}{18}\frac{1}{f_{orb}}\frac{e}{(1-e^2)^{5/2}}\left(1 + \frac{121}{304}e^2\right). \tag{14}$$

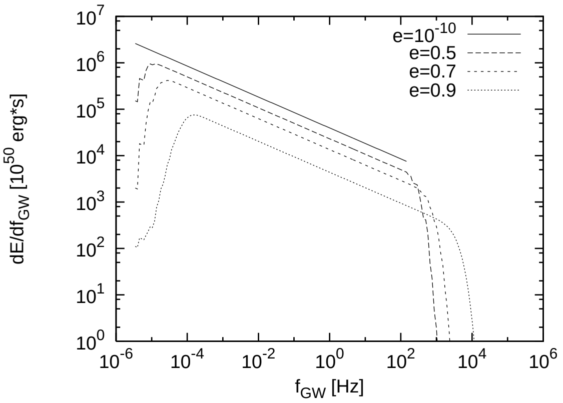

Fig. 3. Spectrum of the GW radiation from short-lived binaries for different values of the initial eccentricity. Solid line corresponds to circular orbit, by dashed line we show case for eccentricity 0.5, dotted line corresponds to eccentricity 0.7 and dash-dotted line to initial eccentricity 0.9

Let us denote the dependence of the eccentricity on the orbital frequency as $e(f_{orb})$.

The gravitational wave spectrum is

$$\frac{dE}{df} = \sum_{n=2}^{\infty} \frac{dE}{df_{gw}^{n}}(e = e(f_{gw}^{n}/n)), \tag{15}$$

where the functions $\frac{dE}{df_{gw}^n}$ are evaluated only for the frequencies in the range $nf_{ini} < f_{gw}^{n} < nf_{ISCO}$.

We illustrate this case with a binary with the same mass as in previous section: $M_1 = M_2 = 300\,M_{\odot}$, but a much tighter orbit $a = 1.2 \times 10^2\,R_{\odot}$. We present the spectra for four different values of eccentricity in Figure 3.

For the case of zero eccentricity the spectrum is a simple power law. For non zero eccentricities the power law spectrum acquires a tail that increases to higher frequencies. The shape of the high frequency tail in the spectrum is determined by value of the eccentricity of the system.

4. Gravitational wave background radiation

We analyze population of the massive black hole binaries using the `StarTrack` population synthesis code (Belczynski et al. 2002). For each system we obtain its component masses $M_{1,i}$, $M_{2,i}$, and its initial orbital parameters: the semi-major axis a_i, and the eccentricity e_i. We denote the total mass of the system as $M_i = M_{1,i} + M_{2,i}$, the reduced mass as $\mu_i = \frac{M_{1,i}M_{2,i}}{M_{1,i}+M_{2,i}}$, and the chirp mass $M_{chirp,i} = \mu_i^{3/5} M_i^{2/5}$.

4.1. Evolution of the orbit

Initial value of semi-major axis is given by synthesis population code and we can use it to estimate the lowest frequency possible for particular binary:

$$f_{i,1} = \sqrt{\frac{GM}{\pi^2 a_i^3}}. \tag{16}$$

Eccentricity and semi-major axis will be changing during the evolution according to two differential equations:

$$\frac{da}{dt} = -\frac{\beta}{a^3}\Psi(e) \qquad \Psi(e) = \frac{1 + 73/24e^2 + 37/96e^4}{(1-e^2)^{7/2}}, \tag{17}$$

$$\frac{de}{dt} = -\frac{19}{12}\frac{\beta}{a^4}\Phi(e) \qquad \Phi(e) = \frac{(1 + 121/304e^2)e}{(1-e^2)^{5/2}}. \tag{18}$$

We have to calculate the size of the orbit after Hubble time. In case of short-living systems we assume final great semi-major axis as $a_f = 10^{-3} R_{\odot}$ (beyond that value we should consider tidal effects). Angular momentum time scale is comparable with age of the binary, so it will merge eventually. In the other case (long-living systems) we have to solve equations (17) and (18). Then, we can calculate frequency corresponding to the final size of the orbit in the same way as we did it for initial parameters.

4.2. Spectrum

A stochastic background is described in terms of present-day gravitational wave energy density (ρ_{gw}) per logarithmic frequency interval normalized to the critical rest-mass energy density ($\rho_c c^2$) Phinney (2001):

$$\Omega_{gw}(f) = \frac{1}{\rho_c c^2}\frac{d\rho_{gw}(f)}{d\ln(f)}. \tag{19}$$

The total present day energy density contained in the gravitational radiation is related to $\Omega(f)$ and amplitude of the gravitational wave spectrum over a logarithmic frequency interval ($h_c(f)$) through:

$$\mathcal{E}_{gw} = \int_0^{\infty} \rho_c c^2 \Omega_{gw}(f)\frac{df}{f} = \int_0^{\infty} \frac{\pi}{4}\frac{c^2}{G} f^2 h_c^2(f)\frac{df}{f}. \tag{20}$$

On the other hand $\mathcal{E}_{gw}$ should be the sum of the energy radiated by all sources at all redshifts.

$$\mathcal{E}_{gw} = \int_0^{\infty}\int_0^{\infty} N(z)\frac{1}{1+z} f_r \frac{dE_{gw}}{df_r} dz \frac{df}{f}. \tag{21}$$

Since Universe is expanding, the observed frequency is different from the emitted and it is equal to $f_r = f(1+z)$, while $N(z)$ is the number of sources in the interval $(z, z+1)$.

Combining (20) and (21) we obtain:

$$\begin{aligned} \rho_c c^2 \Omega_{gw}(f) &= \frac{\pi}{4}\frac{c^2}{G} f^2 h_c^2(f) = \\ &= \int_0^{\infty} N(z)\frac{1}{1+z}\left(f_r \frac{dE_{gw}}{df_r}\right)\Bigg|_{f_r = f(1+z)} dz. \end{aligned} \tag{22}$$

Using (10) we obtain equations describing spectrum from a single harmonic for one type of source:

$$\begin{aligned} \Omega(f_{gw}^n) &= \frac{G^{2/3} M_{chirp}^{5/3} 2^{2/3} \pi^{2/3}}{3n^{2/3}\rho_c c^2} \times \\ &\times (f_{gw}^n)^{2/3}\frac{g(n,e)}{\Psi(e)} N_0 \left\langle (1+z)^{-1/3} \right\rangle, \end{aligned} \tag{23}$$

where N_0 is the density of one type of sources:

$$N_0 = \frac{1}{N_{tot}} f_{bin} n_{pop3}, \qquad f_{bin} = \frac{2}{1 + \frac{1}{f_b}}. \tag{24}$$

The term in the brackets is:

$$\left\langle (1+z)^{-1/3} \right\rangle = \frac{1}{N_0} \int_{z_{min}}^{z_{max}} \frac{N(z)}{(1+z)^{1/3}} dz. \tag{25}$$

In the case of Population III binaries the right hand side integral is trivial, since we assumed that all Population III stars were formed at single redshift $z = 15$. Taking into account very short evolution timescales of massive stars Population III stars, we can assume that the binary compact objects were formed at the same redshift.

In order to obtain the energy density from all simulated objects, we sum over harmonics (index n) and over the total number of binaries (index i):

$$\Omega(f) = \sum_{i=1}^{N} \sum_{n=2}^{\infty} \delta(f - f_i^n) \frac{G^{2/3} M_{chirp,i}^{5/3} 2^{2/3} \pi^{2/3}}{3 n^{2/3} \rho_c c^2} \times \tag{26}$$

$$\times (f_i^n)^{2/3} \frac{g(n,e)}{\Psi(e)} N_0 \left\langle (1+z)^{-1/3} \right\rangle .$$

The amplitude of the gravitational wave spectrum ($h_c(f)$) and the spectral density of the gravitational wave background ($S(f)$) follow:

$$h_c^2(f) = \frac{4\rho_c G}{\pi f^2} \Omega(f) \qquad S(f) = \frac{h_c}{f}. \tag{27}$$

5. Results

We present the resulting gravitational wave background spectrum in Figure 4. The standard model spectrum is shown as the thick continuous line. The shape of the background spectrum is determined by three different factors. In the low frequency regime, below 10^{-5}Hz , the background originates in long lived systems, so the spectrum is basically determined by the distribution of initial parameters of the binaries at the time of formation. In the intermediate region, between 10^{-4}Hz and 50Hz the spectrum is due to the short lived systems that merger within the Hubble time. It has a typical slope of $\frac{2}{3}$, which corresponds to the orbit decay due to gravitational wave emission. At the frequencies above 50Hz the spectrum is determined by the higher harmonics arising due to eccentricity of the binaries. Note that in this work we neglect the merger and ringdown phases which may alter the shape of the background spectrum in the region above 50Hz.

5.1. Dependence on the models

The calculation of the background involved assuming the values of several parameters. In this section we present the dependence of the final result on the choice of those parameters. The list of models is shown in Table 1. In the models B1, B2, C, D1 and D2 we vary the initial mass distributions of the binaries. In model D1 the we have increased the minimum mass of a population III star, while in model D2 we decreased upper end of IMF. Models B1 and B2 have different values of the initial mass function slope, and in model C we draw the two masses in the binary form the same IMF. Models E1 and E2 are characterized by a decreased value of the binary fraction to 0.01 for the first one and 0.001 for the latter one. In models F1 and F2 we place the binaries at different formation redshifts, $z_{form} = 10$ and 20. Finally model G corresponds to the population of circular binaries.

The shape of the gravitational wave background calculated with these different assumptions is shown in Figure 4. The effects if decreasing the binary fraction are simply that of the normalization of the spectrum without altering its shape. Varying the initial mass function can change both the normalization of the spectrum, as well as the shape of the high frequency region. Model D2 has cutoff at frequency 10^{-6} Hz due to the lack of high mass binaries. Drawing the two stars from the same distribution leads to formation of a large number of small mass binaries and the overall level of the spectrum decreases. This is similar to increasing the IMF exponent, see model E2. In the case when the IMF exponent is increased (model E1) the level of the spectrum goes up as there are more high mass binaries. The gravitational wave spectra depend very weakly on the redshift of formation of population III stars, as is clearly seen from equation 27. Finally the effects of eccentricity are demonstrated by model G where all binaries all initially circular. This affects only the high frequency tail of the spectrum.

Table 1. List of models used in the parameter study

Model	Description
A	Standard
B1	Binary fraction decreased to 10^{-2}
B2	Binary fraction decreased to 10^{-3}
C	Star masses drawn independently from same distribution
D1	The minimum mass increased to $50 M_{\odot}$
D2	The maximum mass deceased to $100 M_{\odot}$
E1	The IMF exponent decreased to 1.5
E2	The IMF exponent increased to 3
F1	Formation redshift $z_{form} = 10$
F2	Formation redshift $z_{form} = 20$
G	All binaries are initially circular

It is also intersting to compare the gravitational wave background from population III binaries with the gravitational wave backgrounds from other types of comact binaries. Recently Rosado (2011) performed such a comprehensive calculation. We present the standard model results along with the results of the Rosado (2011) calculation in Figure 5. The lower mass comact object binaries dominate the region above 100Hz. In the region below 100Hz the spectrum of the population III background is an order of magnitude higher than the NSNS background as calculated by Rosado (2011).

From Figure 4 one can see that the gravitational wave background should be clearly detectable with the next generation instruments. ET will detect it, if the binary fraction was larger than 10^{-2}. In the case of LISA, the background would show up just above the threshold in the band around 10^{-3}Hz. However, for future experiments like DECIGO, the gravitational wave background from population III stars could be the dominating noise source even if the binary was as low as 10^{-3}. However, at this level the gravitational wave background from population III stars will be well buried under the background coming from double neutron star binaries formed at later epochs.

6. Summary

We have analyzed the population III metal free binaries. The evolution of such binaries lead to formation of binary black holes, which in turn will be a source of gravitational waves. We calculate the stochastic background from such binaries and show that it can potentially be a significant contribution to the overall gravitational wave background. The spectrum has a characteristic slope of $\frac{2}{3}$ below $\approx$ 50Hz, and is falling of above that frequency.

We have investigated dependence of the shape of the gravitational wave spectrum on the evolutionary parameters of the population III binaries. The evolutionary parameters mainly affect the level of the spectrum, while its shape is rather insensitive to the parametrization. Only in the region above 50Hz, where the spectrum fall off rapidly, the shape of the spectrum varies with the model. In that spectral range the shape is mainly affected by the initial mass function of the population III binaries. For the binary fraction greater than 10^{-2} the gravitational wave background below 100Hz is dominated by the contribution from population III BBH binaries.

The stochastic background from population III BBH binaries should be detectable by the next generation instruments like LISA, DECIGO, and ET. However, the distinctive feature of this background is the break in the region of $50 - 100$Hz. This is unfortunately below the sensitivity of ET. Thus, it will be very difficult to distinguish the origin of the background if detected by any of the above mentioned instruments. A detailed investigation of the spectrum of the gravitational wave background above 50Hz would be most interesting. It could potentially reveal the nature of the sources of gravitational wave background, their mass spectrum, as well as show some effects connected with eccentricity of the binaries. On the other hand lack of detection of the stochastic background will lead to some constraints on the binary fraction and masses of population III binaries.

Acknowledgements. The authors would like to thank Tania Regimbau for carefull reading the manuscript and helpful discussions as well, as Pablo Rosado for providing data from his latest research. This work was supported by the FOCUS 4/2007 Program of Foundation for Polish Science, the Polish grants N N203 302835,N N203 511238, DPN/N176/VIRGO/2009 and the Associated European Laboratory “Astrophysics Poland-France”

References

Abel, T., Bryan, G. L., & Norman, M. L. 2002, Science, 295, 93
Accadia, T., Acernese, F., Antonucci, F., et al. 2011, Classical and Quantum Gravity, 28, 114002
Baraffe, I., Heger, A., & Woosley, S. E. 2001, ApJ, 550, 890
Belczynski, K., Bulik, T., & Rudak, B. 2004, ApJ, 608, L45
Belczynski, K., Kalogera, V., & Bulik, T. 2002, ApJ, 572, 407
Bromm, V., Coppi, P. S., & Larson, R. B. 2002, ApJ, 564, 23
Bromm, V., Kudritzki, R. P., & Loeb, A. 2001, ApJ, 552, 464
Bromm, V. & Loeb, A. 2006, ApJ, 642, 382
Clark, P. C., Glover, S. C. O., Smith, R. J., et al. 2011, Science, 331, 1040
Greif, T. H., Springel, V., White, S. D. M., et al. 2011, ApJ, 737, 75
Heger, A., Baraffe, I., Fryer, C. L., & Woosley, S. E. 2001, Nuclear Physics A, 688, 197
Heger, A. & Woosley, S. E. 2002, ApJ, 567, 532
Kawabe, K. & the LIGO Collaboration. 2008, Journal of Physics Conference Series, 120, 032003
Kulczycki, K., Bulik, T., Belczyński, K., & Rudak, B. 2006, A&A, 459, 1001
Kuroda, K. & LCGT Collaboration. 2010, Classical and Quantum Gravity, 27, 084004
Machida, M. N., Omukai, K., Matsumoto, T., & Inutsuka, S.-i. 2008, ApJ, 677, 813
Marassi, S., Schneider, R., Corvino, G., Ferrari, V., & Portergies Zwart, S. 2011, ArXiv e-prints
Marigo, P., Chiosi, C., & Kudritzki, R.-P. 2003, A&A, 399, 617
Marigo, P., Girardi, L., Chiosi, C., & Wood, P. R. 2001, A&A, 371, 152
Olmez, S., Mandic, V., & Siemens, X. 2011, ArXiv e-prints
Peters, P. C. 1964, Physical Review, 136, 1224
Peters, P. C. & Mathews, J. 1963, Physical Review, 131, 435
Phinney, E. S. 2001, ArXiv Astrophysics e-prints
Regimbau, T. 2011, Research in Astronomy and Astrophysics, 11, 369
Rosado, P. A. 2011, Phys. Rev. D, 84, 084004
Saigo, K., Matsumoto, T., & Umemura, M. 2004, ApJ, 615, L65
Schaerer, D. 2002, A&A, 382, 28
Stacy, A., Greif, T. H., & Bromm, V. 2010, MNRAS, 403, 45
Stacy, A., Pawlik, A. H., Bromm, V., & Loeb, A. 2012, MNRAS, 2251
Tan, J. C. 2008, in IAU Symposium, Vol. 255, IAU Symposium, ed. L. K. Hunt, S. Madden, & R. Schneider, 24–32
Tumlinson, J. & Shull, J. M. 2000, ApJ, 528, L65
Turk, M. J., Abel, T., & O’Shea, B. 2009, Science, 325, 601
Van Den Broeck, C. 2010, ArXiv e-prints
Webbink, R. F. 1984, ApJ, 277, 355
Zhu, X.-J., Howell, E., Regimbau, T., Blair, D., & Zhu, Z.-H. 2011, ApJ, 739, 86

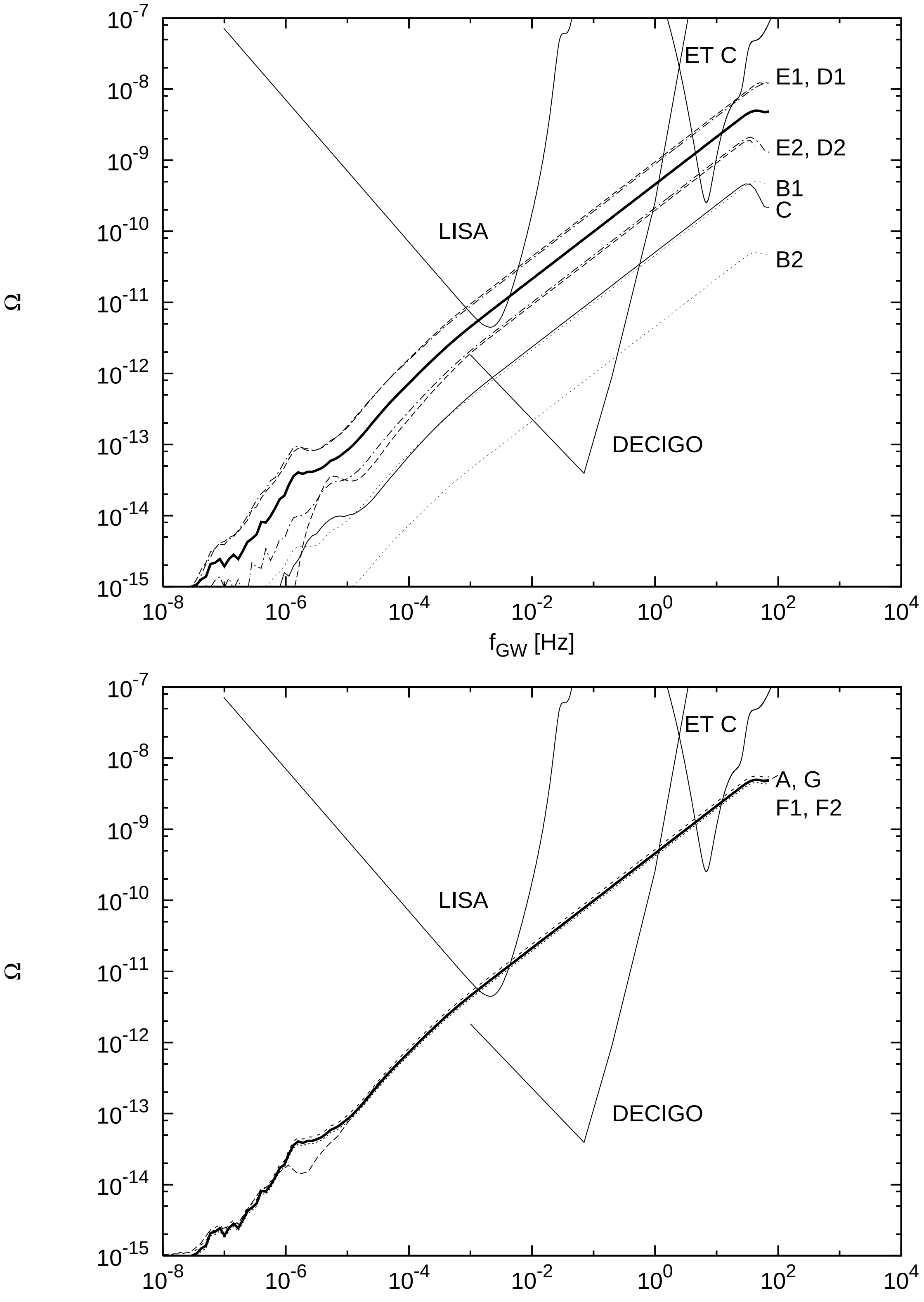

Fig. 4. The gravitational wave background form population III stars. The standard model results are presented as the thick solid line and denoted as A. The thin lines are labeled with a letter denoting the model, for description see Table 1. We also present the sensitivities of future gravitational wave experiments experiments. Bottom panel was created for clarity, because models G, F1 and F2 are no different form the standard model.

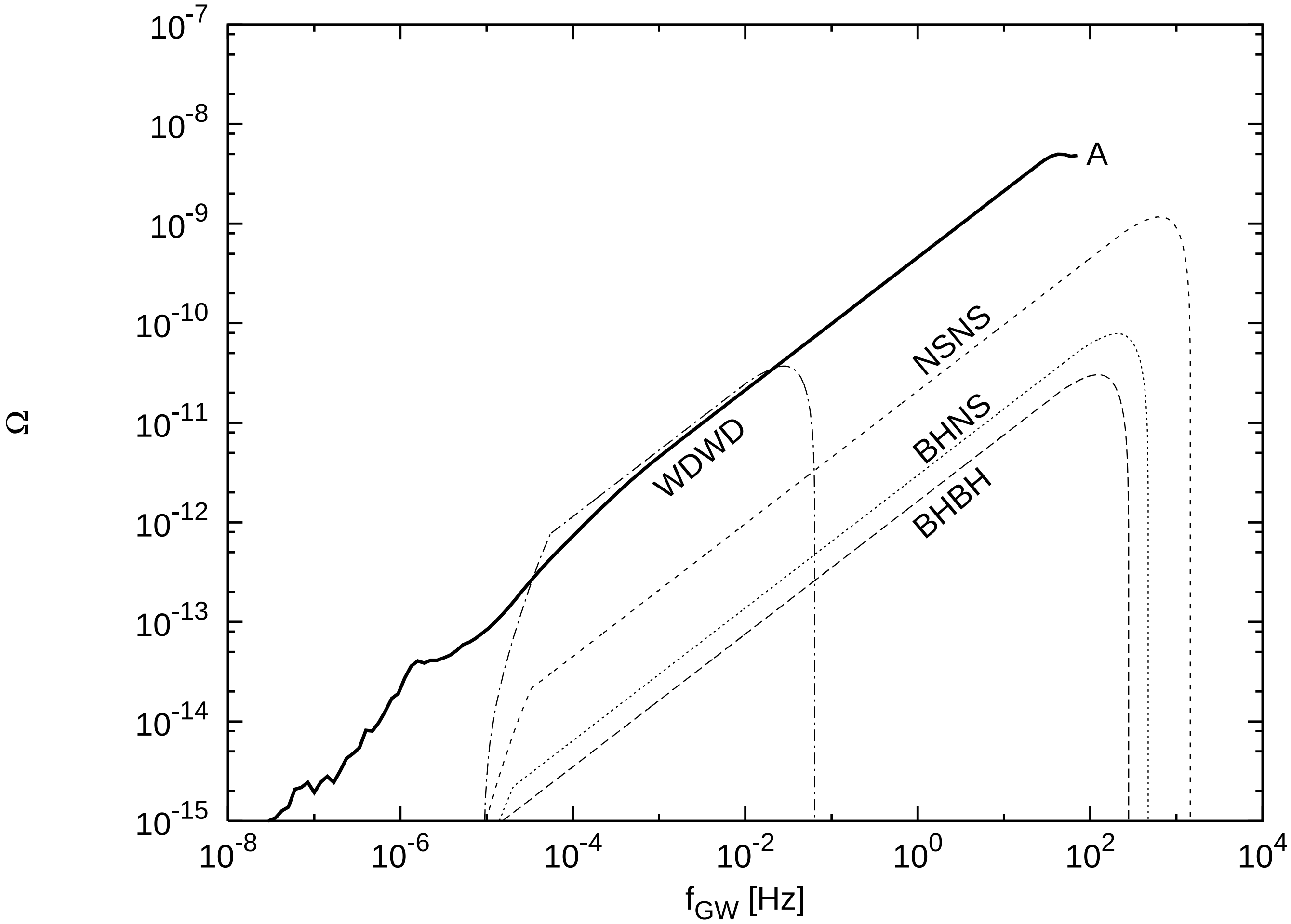

Fig. 5. The gravitational wave background form population III stars. Comparison with the results of Rosado (2011). Solid line corresponds to our standard model A. Dotted and dashed lines are showing background from different classes of compact objects calculated by Rosado (2011).